Journal of the KSTLE Vol. 23, No. 5, October 2007, pp. 240~247
The Korean Society of Tribologists & Lubrication Engineers

Design of Air Turbine and Air Bearing for Dental Handpiece

Pyung Hwang†, Sang Shin Park, Jeong L. Sohn*, Seong In Kwon, Do Hyung Kim** and Woo Seok Kim****

School of Mechanical Engineering, Yeungnam University, Gyongsan, Korea
**School of Mechanical and Aerospace Engineering, Seoul National University*
***Dept. of Mechanical Engineering, Yeungnam University, Gyongsan, Korea*

Abstract – The design process of the dental handpiece is described. The parameters of the high speed air turbine are estimated. The effect of supply hole on the stiffness and damping of the air bearing for handpiece is studied numerically. The Reynolds equation is solved by using the divergence formulation and the perturbation method. The test rig is built and the test procedure is developed for the turbine rotational speed measurement by using Fourier transform of noise generated by the turbine during steady operation.

Key words – dental handpiece, air turbine, externally pressurized air bearing.

1. Introduction

Among various equipment for dental clinics, there is a small drill (usually called a "handpiece") that is used in tooth treatment for making holes, cutting and polishing. The handpiece usually rotates at more than 200,000 rpm. In the tooth drilling machine, the handpiece is attached to the end of the hose that supplies air, water and electricity.

The core of the handpiece is the air-pressure turbine driven by the externally pressurized air and the part consisting of the air bearings that is usually called "cartridge". The air turbine shaft is supported with two coaxial aerostatic journal bearings. The externally pressurized air is used to provide high air bearing stiffness, which helps to prevent resonance at low rotational speeds.

The cartridges with rotation speed above 600,000 rpm are needed in order to decrease the cutting power and the patient's pain, and also to make it possible to complete the treatment in one hour. Another origin of patient's fear is the noise produced by a drilling machine. It urges the development of the manufacture technology of high speed low noise cartridges.

For this purpose, the turbine design, the air bearing design, the rotor vibration, materials and noise reduction should be studied.

Experimental determination of the dental air turbine handpiece characteristics is often required [1,2]. Salma Bahannan et al.[3] studied the noise level of dental handpiece. Dyson and Darvell[2,4] used a fibreoptic tachometer to measure the free running speed.

Numerical analysis is a valuable instrument of the air bearing design. Kawabata[5,6] derived the Divergence Formulation for Boundary Fitted Coordinate System (BFCS), which can be used for gas lubrication analysis at high compressibility numbers and discontinuous film thickness with complicated boundary conditions. Park et al.[7,8] calculated the static and dynamic properties of the externally pressurized bearings considering inherently compensated restrictor.

2. Turbine design

Figure 1 gives the simplified illustration of the air turbine under consideration. There are circumferential blade turbines and radial blade turbines. Since the

†주저자 · 책임저자 : phwang@ynu.ac.kr

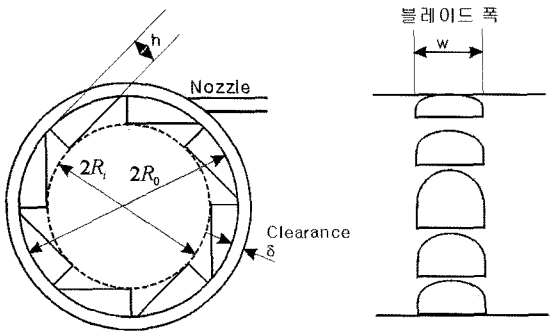

Fig. 1. Base shape of the air turbine.

radial blades require high cost industrial processing, the circumferential blade turbine will be designed.

Denote the internal radius by R_i, external radius by R_o, blade height by h, blade thickness by w, the spacing between the air supply nozzle and the end of the blade by δ.

Consider the aerodynamic properties of the inflow air for one blade.

If U is the circumferential linear speed at the average radius R_m that depends on the rotor angular speed ω, C is the absolute velocity of inflow air at the blade entrance, and V is the relative velocity of the outflow air at the blade outlet, then the outflow velocity will be shown on the right side of the velocity triangle. From this triangle, one can find that the circumferential component of the outflow air speed coincides with the linear circumferential speed U related to the rotor angular speed.

Using the velocity components and applying the basic Euler's equation, the power generated by the turbine can be expressed as follows:

$$\begin{aligned} W &= \dot{m}U(C_{w1}-C_{w2}) \\ &= \dot{m}U(C_{w1}-U) \\ &= \dot{m}R_m\omega(C_{w1}-R_m\omega) \end{aligned} \tag{1}$$

where in is the mass flow rate (kg/s) of the inflow air that flows through the nozzle to the rotor. From the relationship $W=T\omega$, the required torque can be found as follows:

$$T = \dot{m}R_m(C_{w1}-R_m\omega) \tag{2}$$

Assuming that at the blade entrance the inflow air flows in circumferential direction, the inflow air velocity can be found from $in=\rho C_{w1}A_{in}=\rho C_{w1}hw$ as follows:

$$C_{w1} = \frac{in}{\rho hw} \tag{3}$$

Hence, according to above mathematical relationships, the geometrical form and the performance of the turbine can be analyzed in the following order.

1. On the base of the standard atmosphere conditions, under the ideal gas assumptions, the air density is calculated as follows:

$$\rho = \frac{p}{\Re T} \tag{4}$$

where $\Re$ is the gas constant, $287\,J/kgK$. The standard atmosphere conditions are

$p=1$ atm $=101{,}325$ N/m^2,
$T=25$°C$=298$°K

2. The rotor external radius R_o is specified and the internal radius R_i is assumed.

3. The blade width w is specified.

4. The blade height is found as follows:

$$h=K(R_o-R_i) \tag{5}$$

where K is the coefficient determining the blade height. Since the wear is high at $K=1.0$, $K<1.0$ should be chosen when possible. The blade height can also be calculated after the number of blades is specified.

5. The average radius is found.

$$R_m=R_o-0.5h \tag{6}$$

6. The tip clearance between the rotor and the cage, δ, is specified.

7. The objective rotation speed, N (rpm) is specified. Now the rotor angular velocity can be calculated as $\omega=2\pi N/60$.

8. The air flow rate, in, is assumed..

9. The inflow air velocity at the blade entrance is found as follows:

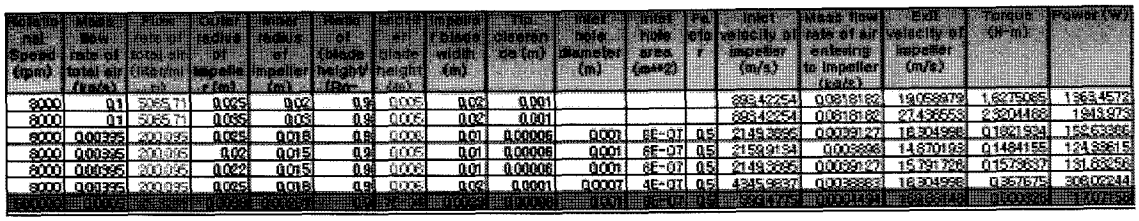

Rotating nal Speed (rpm)	Mass flow rate of total air (kg/s)	Mass flow rate of air (kg/min)	Outlet radius of impeller (m)	Inlet radius of impeller (m)	Width of blade height (m)	No. of blades	Impeller blades width (m)	Tip clearan ce (m)	Inlet hole diameter (m)	Inlet hole area (m**2)	Fa ctor r	Inlet velocity of impeller (m/s)	Mass flow rate of air entering to impeller (kg/s)	Exit velocity of impeller (m/s)	Torque (N-m)	Power (W)
8000	0.1	5065.71	0.025	0.02	0.9	0.005	0.02	0.001				888.42254	0.08181682	19.068979	1.6275085	1363.4572
8000	0.1	5065.71	0.025	0.03	0.9	0.005	0.02	0.001				888.42254	0.08181682	27.436553	2.3204482	1943.973
8000	0.00395	200.035	0.025	0.018	0.8	0.005	0.01	0.00006	0.001	8E-07	0.5	2149.3695	0.00397427	18.304968	0.1821934	152.63986
8000	0.00395	200.035	0.02	0.015	0.9	0.005	0.01	0.00006	0.001	6E-07	0.5	2159.9134	0.0039896	14.870193	0.1484155	124.33815
8000	0.00395	200.035	0.022	0.015	0.9	0.005	0.01	0.00006	0.001	6E-07	0.5	2149.3695	0.00397427	15.791726	0.1573637	131.83256
8000	0.00395	200.035	0.025	0.018	0.9	0.005	0.02	0.0001	0.0007	4E-07	0.5	4345.9837	0.0039896	18.304968	0.357675	300.02244

fig. 2. Calculation of the turbine parameters by using electronic tables.

$$C_{w1} = \frac{in}{\rho(h+\delta)w} \tag{7}$$

10. Considering the loss through the tip clearance, the corrected air mass flow rate entering the blade can be found as follows

$$in_c = in\frac{h}{(h+\delta)} \tag{8}$$

11. The circumferential component of the absolute outflow air velocity at the blade outlet is found as follows:

$$C_{w2} = U = R_m\omega = R_m\left(\frac{2\pi}{60}N\right) \tag{9}$$

12. The torque is found as follows.

$$T = in_c\left(\frac{2\pi}{60}N\right)(C_{w2} - C_{w1}) \text{ (units: Joule)} \tag{10}$$

13. The power is found as follows.

$$W = T\left(\frac{2\pi}{60}N\right) \text{ (units: Watt)} \tag{11}$$

For calculating air turbine characteristics, a simple program was written in Microsoft Excel according to the procedure described above. The calculation results are shown in Fig. 2. At the bottom line of the table shown in Fig. 2 we can see tracks of try and error searching of the design values for specified rotation speed of 500,000 rpm, air flow below 25. liter/min, and required dynamic power above 1 W. Setting R_o=3.6 mm, R_i=2.81 mm, blade height h=0.79 mm, diameter of supplier of 0.2 mm, and designing the impeller in such a way to provide a power of 1 W, the number of nozzles required for such impeller calculated on the basis of Bernoulli equation are shown in a table in Fig. 3.

The following should be taken into consideration when designing the rotor.

1. For manufacturability, the perpendicular rotor blade shape is appropriate. (The above theory and calculation method were based on the perpendicular blade shape.) In order to improve the operating efficiency, the perpendicular section of the blade must be inclined forward with respect to radial direction.

2. In order to avoid the frangibility of the blades ends, it should not be sharp. In this case, there is no meaning in calculation procedure for rotor internal radius R_i.

3. The number of rotor blades must be chosen adequately. Although there are good points in increasing the blades number, if the inflow velocity is increased due to decreasing the blade height, such effects as the air compressibility must be taken into account; and also, the manufacturing cost is increased.

4. The radius of the air supply nozzle should be determined to maximize the nozzle cross-section within the blade perpendicular section. The attention should be paid to the similarity of the nozzle cross-section and the blade perpendicular section, which helps to avoid the situation when the air inflows onto the lower blade. In the case of nozzle cross-section smaller than the blade perpen- dicular

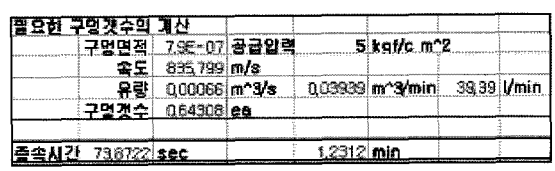

필요한 구멍갯수의 계산						
구멍면적	7.9E-07	공급압력	5	kgf/c m^2		
속도	835.799	m/s				
유량	0.00066	m^3/s	0.03939	m^3/min	39.39	l/min
구멍갯수	0.64308	ea				
충속시간	73.6722	sec	1.2312	min		

Fig. 3. Calculation of the number of holes.

section, the nozzle should be positioned in such a way that for the blade put in radial position the nozzle upper end is located at the blade bottom end. If the blade end is higher, considerable amount of inflow air will flow out through the tip clearance instead of pushing the blade.

5. The width of the rotor blade should be chosen appropriately within the safe range. However, when the blade width is too narrow the power is decreased due to decrease of the inflow velocity.

6. Choosing the tip clearance as small as possible is good for efficient work of the rotor.

7. Choosing the light material for the rotor is good for minimizing initial inertia force.

8. Due to inertia force and various losses, the safe arrangement of air flow requirement is slightly higher than the calculation result.

3. Air bearing design

An arbitrary axisymmetric lubricated fluid film is considered, as shown in Fig. 4. The coordinates (r,θ,z) are cylindrical coordinates and s is the meridian coordinate. The arbitrary coordinate system (ξ,η) is considered for the air film surface. The coordinates (ξ,η) are parallel to boundaries where the air film height varies successively. In the computational domain, the coordinates (ξ,η) form a rectilinear grid with intervals equal to 1.

The air flow rates in meridian and circumferential directions are expressed as

$$q^s = -\frac{\rho h^3}{12\mu}\frac{\partial p}{\partial s} \tag{12}$$

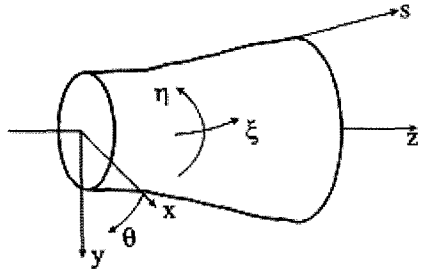

Fig. 4. Arbitrary lubricated surface.

$$q^s = -\frac{\rho h^3}{12\mu r}\frac{\partial p}{\partial s} + \rho h r\bar{\omega}$$

where ρ is the air density, h is the air film thickness, μ is the air viscosity, p is the air pressure, r is the bearing radius and

$$\bar{\omega} = (\omega_1 + \omega_2)/2 - \omega_r \tag{13}$$

ω_1 and ω_2 are the rotational speeds of the shaft and bearing, and ω_r is the rotational speed of the coordinate system.

In the case of isothermal flow, the air density ρ is proportional to the air pressure.

The effect of the external pressurization is given by the supply flux at the nodes corresponding to orifices

$$q_{sup} = C_D \pi d_s h \sqrt{R p_s}\,\Phi \tag{14}$$

where C_D is the dispersion coefficient of the pipe flux, d_s is the flow supply pipe diameter, h is the steady state film thickness, $R = 1/(\Re T)$, $\Re$ is the gas constant, T is the temperature, p_s is the supply pressure, and Φ is a-function of the gas adiabatic constant χ.

The function Φ has two states, depending on the ratio of pressure under compensator and supply pressure

$$\text{for } \frac{p}{p_s} \le \left[\frac{2}{x+1}\right]^{x/(x-1)}$$

$$\Phi = \left[\frac{2x}{x+1}\right]^{1/2}\left[\frac{2}{x+1}\right]^{1/(x-1)}, \tag{15}$$

$$\text{for } \frac{p}{p_s} \le \left[\frac{2}{x+1}\right]^{x/(x-1)}$$

$$\Phi = \left[\frac{2x}{x-1}\right]^{1/2}\left[\left(\frac{p}{p_s}\right)^{2/x} - \left(\frac{p}{p_s}\right)^{(x+1)/x}\right]^{1/2}, \tag{16}$$

The algebraic equations for the air pressure are obtained applying the flux balance condition to the control volume around each air node. The air bearing stiffness and damping are calculated using the perturbation method. The details of the numerical method can be found in[5,6,7,8].

Although at the location of the journal bearings

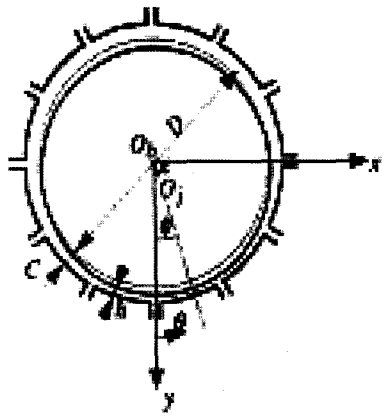

Fig. 5. Orifice type externally pressurized journal bearing.

the turbine outer radius is designed to be 7.2 mm, actually, it is slightly smaller. The reason for this is that the blade height constitutes only 90% of the difference between the inscribed and circumscribed circles. So, for smooth assemblage of the shaft and the bearing, the bearing radius is decided to be 5 mm. In order to maintain the bearing length to radius ratio equal 1 : 1, the bearing length was also fixed at 5 mm. The air supply orifices are located in two rows, 8 orifices in each row in circumferential direction.

Figure 5 shows an example of the orifice-type journal bearing, and Fig. 6 shows an example of the air pressure calculation for 12 orifices posi- tioned in two rows.

The choice of the bearing clearance is very important. Too small clearance leads to the stability problem, while too big clearance makes it difficult to achieve the required stiffness. In the present work, the clearance was fixed at 8 mm. The air bearing stiffness and damping were calculated for a range of the flow supply pipe diameter.

Figure 7 shows the air bearing stiffness, and Fig. 8 shows the air bearing damping. The air bearing stiffness is increased successively with the pipe radius, and decreases abruptly after the radius achieves 0.2 mm. However, the air bearing damping constantly decreases with increasing the pipe radius. In order to provide enough damping at high

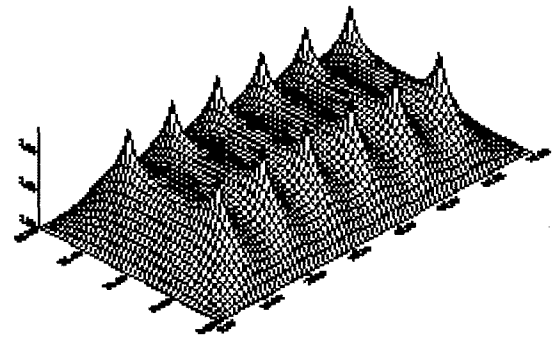

Fig. 6. Pressure distribution for orifice type externally pressurized journal bearing.

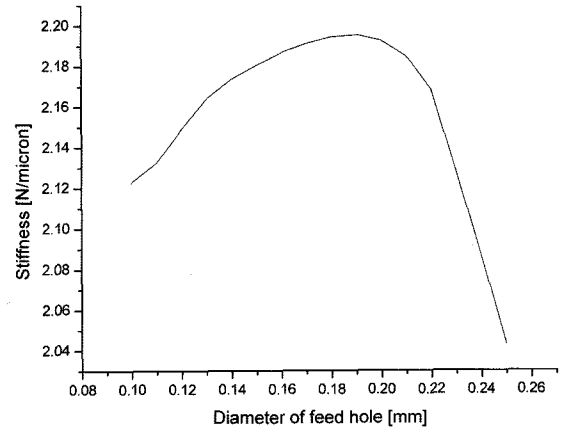

Fig. 7. Air bearing stiffness.

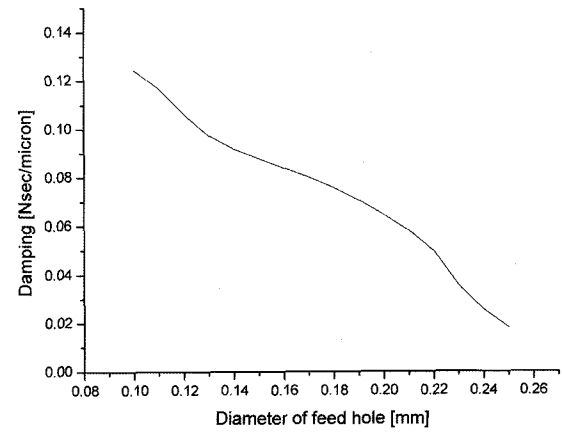

Fig. 8. Air bearing damping.

rotational speed, the pipe radius was chosen to be 0.15 mm.

Computer Aided Design software was employed to

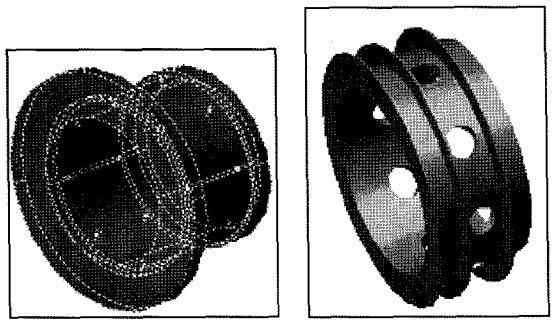

Fig. 9. Model of the air bearing. (a)-Internal part; (b)-External part.

model the components of the air turbine and their assemblage. Figure 9 (a) shows the internal part of the bearing that supports the shaft of the dental air turbine. It is one of the core parts of the turbine, and it should pass though several processing stages. The external part of the bearing shown in Fig. 9 (b) has a shape of a very thin belt. The components shown in Fig together constitute a complete bearing. Assembling the bearing requires a high precision jig for insertion and adjustment. A care should be taken to avoid application of excessive force or impact that can result in a deformation. After the two parts are assembled, a pocket shape pipeline that provides uniform pressure and uniform flow rate in circumferential direction should be made. The high air pressure is generated in the pockets due to air supply through the small holes that can be seen in Fig. 9 (a).

Figure 10 shows the model of the turbine shaft. For the medical treatment, the dental tools are installed in the hole in the shaft center. In order to provide exact clearance between the shaft and the bearing, accurate shaft processing is required. The turbine blades should be designed to provide maximum action of the compressed air and should be processed with special care, because this part has a big influence on the turbine rotational speed.

Figure 11 shows all components described above in assembled state, and Fig. 12 shows the assemblage process. At this stage, two identical outside

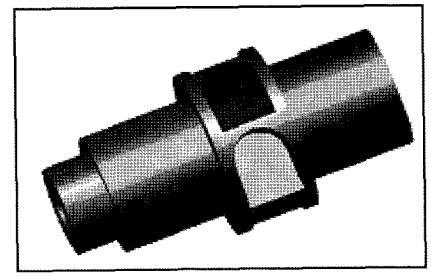

Fig. 10. Model of the turbine shaft.

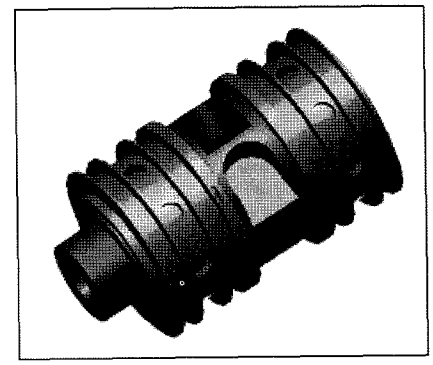

Fig. 11. Assembled air turbine.

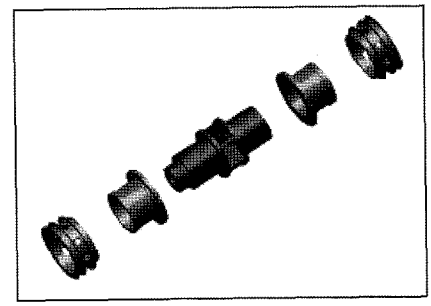

Fig. 12. A deal drawing of the turbine system.

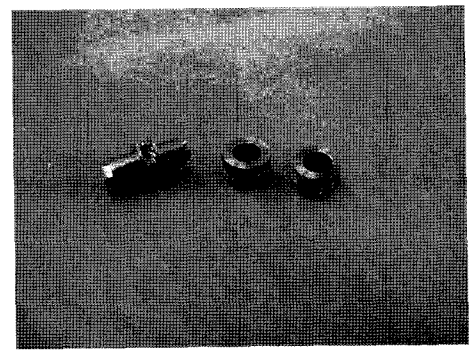

Fig. 13. Manufactured turbine shaft and bearings.

Fig. 14. Rotational speed test rig.

details should be sealed with an O-ring.

Figure 13 shows the manufactured air turbine and bearings.

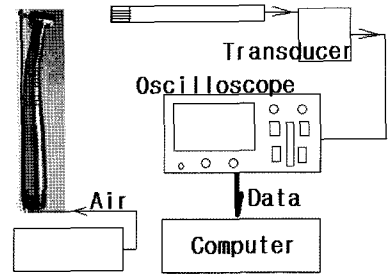

Fig. 15. Signal processing flow chart for the rotational speed test.

4. Turbine rotation speed measurement

For the purpose to measure the rotation speed of high-speed dental air turbine, the experimental rig was constructed as shown in Fig. 14. The measuring range of usual device such as tachometer is not

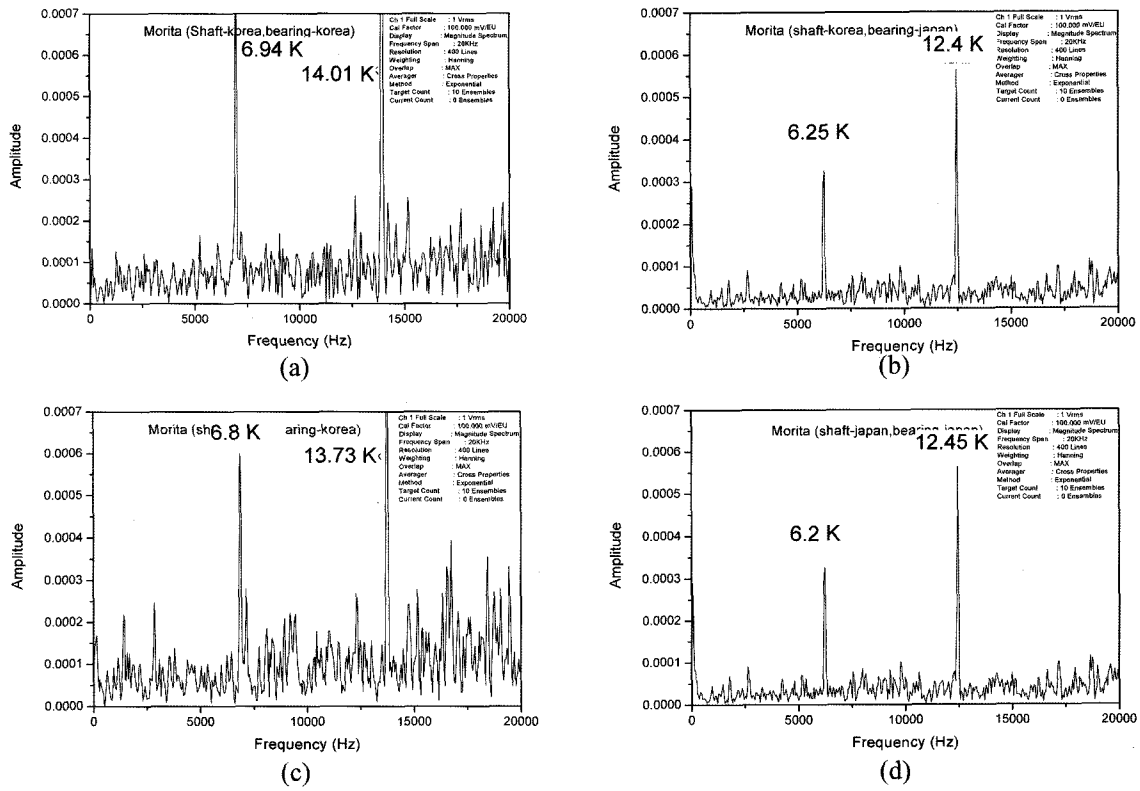

Fig. 16. Power spectrum of the operational noise of the air turbine.
(a) The shaft and the bearings are made in Korea;
(b) The shaft is made in Korea and the bearings are made in Japan;
(c) The shaft is made in Japan and the bearings are made in Korea;
(d) The shaft and the bearings are made in Japan.

that reason, the noise generated during rotation was measured.

The measured signal passes through a converter and appears at oscilloscopes in a waveform (Fig. 15). This waveform is very complicated, and generally the accuracy of the signal is not enough to analyze by using the time-domain methods.

After the system sets in a steady state, a part of the signal which is shown by oscilloscopes is saved to a file. Then the Fourier transform is used to find the main frequency components of the rotation noise.

The turbine frequency was measured for four kinds of MORITA handpieces. The results are given in Fig. 16. The first peak in the power spectrum is between 6 and 7 kHz (360,000-420,000 rpm). The second peak corresponds to the two times higher frequency. We can see that the turbine with the shaft and the bearings both made in Korea has the highest rotational speed, although the total difference is within 17%. Two handpieces with Japan-produced bearings have lower noise level. The comparison shows that the choice of the bearings plays the primary role for the rotation speed and noise level.

5. Conclusions

The dental handpiece air turbine design including the turbine blades, nozzles, and the air bearing is developed. The procedure of the turbine parameters calculation is presented. The pressurized air supply pipe radius is chosen on the base of numerical calculation of the air bearing stiffness and damping.

The test rig for high-speed dental air turbine is constructed. The turbine rotation speed is measured by using the Fourier transform of the vibration that is generated during steady rotation.

This research is sponsored by 2003/2004 Yeungnam University Research Fund after ITEP Program.

References

1. Brockhurst, P. J. and Shams, R., "Dynamic Measurement of the Torque-Speed Characteristics of Dental High Speed Air Turbine Handpieces," Australian dental journal, Vol. 39, No. 1, pp. 33-41, 1994.
2. Darvell, B. W. and Dyson, J. E., A Testing Machine for Dental Air-Turbine Handpiece Characteristics: Free-Running speed, Stall Torque, Bearing Resistance, Federation of operative dentistry, Vol. 30, No. 1, pp. 26-31, 2005.
3. Salma, B., Ahmed, A., E.-H. and Ahmed, B., Noise Level of Dental Handpieces Next Term and Laboratory Engines, The Journal of Prosthetic Dentistry, Vol. 70, Issue 4, pp. 356-360, 1993.
4. Dyson, J. E and Darvell, B. W., Flow and Free Running Speed Characterization of Dental Air Turbine Handpieces, Journal of Dentistry, Vol. 27, pp. 465–477, 1999.
5. Kawabata, N., A Study on the Numerical Analysis of Fluid Film Lubrication by the Boundary-Fitted Coordinates System (The Case of Steady Gas-Lubrication), JSME Int. Journal, Vol. 32, No. 2, pp. 281-288, 1989.
6. Kawabata, N., A Useful Numerical Analysis Method for the Dynamic Characteristics of Fluid Film Lubrication (The case of Incompressible Fluid Lubrication), JSME Int. Journal, Vol. 34, No. 1, pp. 91-96, 1991.
7. Park, S. S. and Han D. C., Measurement of Perturbed Pressures under Inherently Compensated Restrictors in Externally Pressurized Air Bearings, J. of KSTLE, Vol. 12, No. 1, pp. 47-55, 1996.
8. Park S. S., Ahn, Y. and Han, D. C., Analysis of the Air Journal Bearings with Two Circumferential Grooves, J. of KSTLE, Vol. 13, No. 4, pp. 40-46, 1997.